ISSN 2063-5346

MOLECULAR DOCKING STUDIES OF β-AMYLOID PROTEIN WITH NATURAL MULTIPLE LIGANDS OF CHRYSAMINE G, CURCUMIN, THIOFLAVIN T AND TRI PHOSPHONIC ACID: A NOVEL TARGET FOR ALZHEIMER'S DISEASE (AD)

K Ganesh Kadiyala[1*], K. Jagadeesh[1], D.B.N. Suresh Varma[1], B. Kanaka Durga[1], T D L Suneetha[1], Kiranmai Devi[1]

Article History: **Received:** 01.02.2023 **Revised:** 07.03.2023 **Accepted:** 10.04.2023

Key Words: Molecular Docking, β-amyloid, Chrysamine G, Curcumin, Thioflavin T and Tri phosphonic acid, Alzheimer's Disease (AD).

[1] Department of Chemistry, Shri Vishnu Engineering College for Women, Bhimavaram, Andhra Pradesh, India.

DOI: 10.31838/ecb/2023.12.s1.090

Background:

Alzheimer's disease is one of the most prevalent age-linked neurodegenerative conditions afflicting older people. (AD).[1,2] The main risk factor for the development and worsening of AD is age, and the risk almost doubles every five years in adults over 65. [3–5] Over 4.4 crores of people were thought to be affected by this neurological condition in 2015, according to estimates. Nonetheless, it is anticipated that by 2050, this number would have doubled.[6,7] A complicated illness that is genetically predisposed and ecofriendly variables play a substantial role in the pathology, it is revealed that the majority of AD patients (over 95%) either SAD (sporadic AD) or LOAD (late-onset AD).[8,9] On the other side, familial AD or early-onset AD (EOAD) are only detected in less than 5% of AD patients (FAD). It has been discovered that mutations in either of the presenilin-1 (PSEN1), presenilin-2 (PSEN2), and amyloid precursor protein (APP) genes could induce the aforementioned forms of AD (i.e., EOAD and FAD). [10–12]

Abnormal amyloid beta (A) peptide buildup in amyloid plaques and hyperphosphorylated tau clustering in intracellular neurofibrillary tangles are among the neuropathological features of AD (NFTs).[13-16] Additionally, it was found that microglial activation, associated astrogliosis, neuropil threads, and dystrophic neurites (DNs) frequently coincide.[17-18] These pathogenic pathways' after-effects include neurodegeneration with loss of synapses and neurons, which can result in macroscopic atrophy.[19] Studies have revealed that AD-related brain changes could begin even 20 or more years before any symptoms even manifest.[20-23] It has been discovered that when the early changes occur, the brain makes up for them and enables people to carry on with their daily lives regularly. The ability of the brain to make up for the adjustments as the neuronal damage increases, though, and patients start to show modest cognitive diminishing.[24] Far ahead, neuronal damage is so severe that individuals experience obvious cognitive impairment, counting signs like loss of memory or confusion about the time or location.[25,26] The medications that are now on the market only treat symptoms; they are unable to slow the progression of AD.[27,28] Therefore, it is crucial to create medications that can both stop the degenerative processes linked to AD and slow down and sometimes stop the development of the illness. It's interesting to note that the overall prevalence of AD would decrease by 40% if it could be stopped or postponed for five years.[29] Aβ has come to be recognized as the primary treatment target for AD throughout time.[30-32] Also, several pharmaceutical/biopharmaceutical companies are working to create beneficial substances (such as tiny molecules or immunotherapies) that will reduce the buildup of Aβ and maybe improve AD pathogenesis.

Nowadays, the ability to pinpoint specific biological targets has significantly increased in various domains like genetics, biochemistry, molecular biology, and pharmacology. Recently, similar targets have been investigated using computational methods for developing new medications to treat disease. The most popular computational tools for identifying Alzheimer's disease targets are docking and molecular dynamics. Finding out how medications and targets interact at the molecular level is made simpler using the aforementioned tools.

Chrysamine-G (CG) is a histologic marker for amyloid that is a carboxylic acid analogue of Congo red. It partitions into the brain of healthy rodents and binds to the beta-amyloid protein associated with AD in vitro. Its nature is Lipophilic, the Congo red analog, which was demonstrated to attach to the -amyloid protein in vitro. The neurodegenerative action of the -amyloid protein is inhibited by CG through binding to it. Chrysamine-G's antioxidant action prevents amyloid from forming. The blood-brain barrier is crossed by CG, making it an effective probe for finding amyloid clumps. Alternative names of CG were Brasilamina, Yellow G , C.I., Direct Yellow 1, Chrysamine, its PubChem CID was 160843, IUPAC name was 5-[[4-[4-[(3-carboxy-4- hydroxyphenyl) diazenyl] phenyl]phenyl] diazenyl]-2-hydroxybenzoic acid, its Molecular Formula $C_{26}H_{18}N_4O_6$. CG shows a count of 4 Hydrogen Bond Donors, a count of 10 Hydrogen Bond Acceptors, and a count of 7 rotatable bonds.

Due to its therapeutic characteristics, curcumin has generated a lot of attention and research over the past few decades. It is a powerful anti-inflammatory compound, reduces the

inflammation and sometimes potentially it will be used to cure cancer, according to research. Curcumin has been discovered to diminish the transformation, proliferation, and spread of tumours by controlling transcription factors, growth factors, protein kinases, and other enzymes. The two tautomeric forms of curcumin are keto and enol. Both in the solid and solution phases, the enol form is more stable. As it combines with boric acid to create the red chemical rosocyanine, curcumin can also be used to measure boron. Turmeric is frequently ingested in Asian nations and has long been used medically. The curry spice turmeric contains a dietary polyphenol called curcumin, which has powerful anti-inflammatory and antioxidant capabilities as well as the capacity to modify a number of targets thought to be involved in the advance of chronic disease. Curcumin has proven therapeutic potential for treating Parkinson's disease (PD) and Alzheimer's disease (AD), two neurodegenerative conditions. In the ageing brains of several animal species, as well as in an AD sufferer, the binding of curcumin to SPs and cerebral amyloid angiopathy (CAA) as well as its binding to NFTs were studied. Anti-amyloid β protein 1-42 (Aβ42) and anti-amyloid protein 1-40 (Aβ40) antibodies were used to immunostaining brain slices.

The counterion of thioflavin T is 2-[4-(dimethylamino)phenyl]-3,6-dimethyl-1,3-benzothiazol-3-ium. It is frequently used to detect the existence of amyloids, both in vitro and in vivo, and to quantify their presence. It has a role as a fluorochrome and a histological dye. It contains a thioflavin T cation. inhibits the reaction thioflavin T binds to ACHE protein, Binding affinity to beta amyloid protein 1-40 by fluorescence titration. Amyloid fibrils can be recognised both ex vivo and in vitro using the benzothiazole pigment thioflavin T. When it binds to amyloid fibrils, its luminescence is enhanced. It was found that thioflavin T can be found in micelles in solutions of water at fluorescence assay monitoring amounts (between 10 and 20 M). Thioflavin T concentrations were varied, and specific conductivity variations were observed. The critical micellar concentration was determined to be 4.0± 0.5 M. It's interesting to note that variations in the creation of micelles also had an impact on the excitation and emission of thioflavin T fluorescence. Using atomic force microscopy, the 3 nm-diameter thioflavin T micelles were directly detected, and bound thioflavin T micelles were seen along the length of sample fibrils.

The phosphonic acid ATMP, also known as aminotris(methylenephosphonic acid), has the chemical formula $N(CH_2PO_3H_2)_3$. Chelating abilities are present. It can be produced in a manner like the Kabachnik-Fields reaction using the Mannich-type reaction with ammonia, formaldehyde, and phosphoric acid as chemicals. By its superior chelating capacity, low threshold inhibition, and lattice distortion mechanism, ATMP performs better against scale than polyphosphate. In water systems, it can stop the production of scale. Nitrilotriacetic acid's phosphonate analogue is called ATMP.

We concentrated on the function of SPs in the current research and cerebral amyloid angiopathy (CAA) based novel molecules of Chrysamine G, Curcumin, Thioflavin T and Tri phosphonic acid docked with β-amyloid protein and its act as therapeutic targets for AD.

Results

Validation and docking study of crystallographic structure of β-amyloid protein (PDB ID: 2LMN) of homo sapiens and Chrysamine G, Curcumin, Thioflavin T and Tri phosphonic acid inhibitors.

The pdb.qt files were moved using autogrid, docking cycles were set to 50, and finally, the dock log records were examined for any limiting modifications. The ligand record had to be recorded in PDBQT design for AutoDock 4.2/ADT to be used for any docking calculations. PDBQT design is essentially the same as PDB design but includes AutoDock atom kinds ('T') and halfway charges ('Q'). Each atom in the ligand has its own line, and there are distinctive catchphrases that show which atoms, if any, will be flexible during the AutoDock exploration. Processing of ligands includes guaranteeing that its atoms are allowed the right AutoDock particle types (Fig 1). If necessary, Gasteiger charges should be added, non-polar hydrogens should be blended, sweet-smelling carbons should be identified, and the "twist tree" should be set up. Docking pdb.qt documents of receptor were set up by adding all Kolman charges and checking absolute charges

on constructions, as well as adding all polar hydrogens and changing Histidine hydrogens in protein pdb files. The pdb.qt files were moved using autogrid, and the number of docking runs was set to 10. Finally, the dock log entries were checked for limiting compliance.

Examination was based on the free energy of restricting, the energy with the lowest docked value, and calculated RMSD values. (Table 1).

Table 1. Docking results of multiple ligands (Chrysamine G, Curcumin, Thioflavin T & Tri phosphonic acid) molecules docked on to β-amyloid protein 2LMN.

S. No	Lead Molecule	Target Protein	Number in cluster	RMSD from reference structure (A^0)	Estimated Free Energy of Binding (kcal/mol)	Docked energy (kcal/mol)	Estimated Substrate. Conc., Ki uM or mM (micro/millimolar) [Temp= 298.15K]	Catalytic residues
1.	Chrysamine G	β-amyloid	07	0.193	-3.73	-9.03	62.25 uM	Glu-11 Val-12 His-13 His-14
2.	Curcumin	β-amyloid	3	0. 175	-4.45	-9.24	98.25 uM	Leu-17 Val-18 Phe-19 Phe-20 Ala-21 Glu-22
3.	Thioflavin T	β-amyloid	17	0.188	-4.96	-8.57	25.10 mM	Val-12 His-13 His-14
4.	Tri phosphonic acid	β-amyloid	25	0.768	-5.75	-8.25	32.54 uM	Glu-11 Val-12 His-13 His-14

The top atom-docked all-out bunch of docking adaptation displayed negative restricting energy. The total of four energy components, including intermolecular energy (vanderwaal, hydrogen bond, desolvation, and electrostatic energy), absolute interior energy, torsional free energy, and unbound framework energy, is used to calculate the free energy of restriction. We led docking reproduction of sub-atomic communications between crystallographic

construction of and Chrysamine G, Curcumin, Thioflavin T and Tri phosphonic corrosive. Chrysamine G shows the anticipated assessed free energy of restricting -3.73 kcal/mol, docked energy -9.03 kcal/mol to the construction of with assessed substrate conc. Ki 62.25 uM (micro molar) at the temperature of 298.15 K (Fig. 3).

Curcumin shows the anticipated assessed free energy of restricting - 4.45, docked energy -9.24 kcal mol^{-1} to the design of with assessed substrate conc. Ki 98.25 uM (micro molar) at the temperature of 298.15K (Fig. 4).

Thioflavin T shows the anticipated assessed free energy of restricting -4.96 kcal/mol, docked energy -8.57 kcal/mol to the design of with assessed substrate conc. Ki 25.10 mM (milli molar) at the temperature of 298.15 K (Fig. 5).

Tri phosphonic corrosive shows the anticipated assessed free energy of restricting -5.75 kcal/mol, docked energy -8.25 kcal/mol to the design of with assessed substrate concentration (K_i) 32.54 uM at the temperature of 298.15 K (Fig. 6).

Discussion

Docking examination of crystallographic construction of β-amyloid protein with PDB ID: 2LMN and Chrysamine G, Curcumin, Thioflavin T and Tri phosphonic corrosive collaboration shows and empowered us to recognize explicit four buildups Glu-11, Val-12, His-13 and His-14. From the outcomes it has been plainly seen that Curcumin framed four hydrogen bond collaborations which appeared in Fig. 5. Docking investigation with ligand empowered us to recognize explicit buildups viz. Glu-11, Val-12, His-13 and His-14 inside the design of restricting pocket to assume a significant part in ligand restricting partiality. The docking compliance Tri phosphonic corrosive gave the best anticipated restricting free energy of -5.75 kcal/mol to the design of with K_i 32.54 uM at the temperature of 298.15 K for bunch rank one determined using LGA. The distinctive surface pocket buildup is by all accounts a significant factor in deciding the diverse method of ligand connection with construction of Glu-11, Val-12, His-13 and His-14 amino corrosive deposits; it assumed a fundamental part in restricting the bunch of ligands with receptors. These links result from either the configuration of hydrogen bonds or from the establishment of Vander Waals powers. The protein with ligands of Chrysamine G, Curcumin, Thioflavin T, and Tri phosphonic corrosive is in opposition to the restricting mode and liking. Examining the limiting methods of the mixtures Chrysamine G, Curcumin, Thioflavin T and Tri phosphonic corrosive, in the docking reenactment find with under 2 °A RMSD to its docking structure. The outcomes are recorded in table-1. The docking of crystallographic design of β-amyloid protein 2LMN and Chrysamine G, Curcumin, Thioflavin T and Tri phosphonic corrosive, appeared in Graphical theoretical. Our in-silico tests show that Chrysamine G, Curcumin, Thioflavin T and Tri phosphonic corrosive ties β-amyloid, and furthermore it itself represses its capacity and in this way may go about as a medication.

Methods

All computations were executed on a workstation AMD Opteron Dual-Core (2.0 GHz) with 4 GB RAM. Docking estimations were executed with AutoDock 4.2. If not in any case expressed, default settings were utilized during all estimations. Molecular Graphics Laboratory (MGL) devices, Cygwin c:program, and Python 2.5 were simultaneously obtained from www.cygwin.com, the Python 2.7 language from www.python.com, and AutoDock 4.2 from www.scripps.edu.

Docking:

Preparation of Protein

From the PDB, the X-ray crystallographic structure of the homo sapiens -amyloid protein (PDBID: 2LMN) resolved at 2.0 Å[33] was taken for use in the investigation. Prior to the docking simulation, water molecules were taken out of the protein, polar hydrogen atoms were added, and non-polar hydrogen atoms were combined for the correct charge computation. For the ligands of chroysamine G, curcumin, thioflavin T, and triphosphonic acid, Gasteiger charges were given. Using the Python module included with the AutoDock Tools, ligand files were processed concurrently. The ligand files were given Gasteiger charges after which the resulting file was compounded, processed, and

changed into PDBQT format, which is the input format for AutoDock4.2.

Ligand Preparation

The ligands Energy minimization and Preparation of Ligands in AutoDock 4.2 were used to generate Chrysamine G, Curcumin, Thioflavin T, and Triphosphonic acid from grin strings for docking investigations. Using "LigandFit" in AutoDock 4.2, the optimised ligand molecules were docked into the refinement of the -amyloid protein. Semi-flexible docking employed a stiff receptor and a flexible ligand. "PyMol" was used to create all the structural pictures of the proteins and ligands.

Molecular docking

The molecular docking tool used for the docking calculations was the AutoDock 4.2 suite. Using the AutoDock 4.2 software, ligand binding was examined to the X-ray crystallographic structure of β-amyloid[33] using a default grid spacing of 0.375 Å and the grid points in X, Y and Z axis were set to 60 × 60 × 60 Å. The search was based on the Lamarckian genetic algorithm[35] and the results were analyzed using binding energy. For each ligand, a docking experiment consisting of 100 stimulations was performed and the analysis was based on binding free energies and root mean square deviation (RMSD) values, and the ligand molecules were then ranked in the order of increasing docking energies. In order to observe how the docked compound interacted with the crystallographic structure of beta-amyloid, the PMV 1.4.5 viewer was used to perform substrate docking with natural plant substrates from the sterol family of Chrysamine G, Curcumin, Thioflavin T, and Tri phosphonic acid. After docking, the ligand–receptor complexes were analyzed by the PyMOL program.[38]

Active site analysis

A limited number of highly conserved residues in the active site of an enzyme drive its catalytic activity, and these residues are still present in enzymes from unrelated species. Locating and identifying conserved active site residues and providing coherence to the homology model were made possible by superimposing the three-dimensional model with a template to identify the active site. The information on the active site for a template structure was given by the Catalytics Site Atlas (CSA) database of the European Bioinformatics Institute (http://www.ebi.ac.uk/thorntonsrv/databases/CSA/).[34]

Dynamic site investigation

The synergist movement of a chemical is performed by few exceptionally moderated buildups inside the dynamic site, and it stays preserved among remotely related catalysts. Using a layout to superimpose a three-dimensional model on gave the homology model accuracy and made it easier to identify and pinpoint the location of the conserved deposits from the dynamic site. For the purpose of a format structure, information about the dynamic site was obtained from the Catalytics Site Atlas (CSA) data source of the European Bioinformatics Institute (http://www.ebi.ac.uk/thorntonsrv/data sets/CSA/).[33]

Conclusion

Characteristic mixtures have assumed a significant part in pick up the check and forestalling human diseases. We have recognized the possible enemies of Alzheimer's mixtures by focusing on the explicit catalysts which are essential for its endurance. Our computational methodology has given a chance to distinguish characteristic items with a potential antileishmanial movement for test approval, and to comprehend their impacts on Alzheimer's disease framework. The recognized compound from common sources is a possible drug against Alzheimer's disease. The current investigation additionally calls attention to capability of normal assets as helpful specialists. Our examinations demonstrate that Chrysamine G, Curcumin, Thioflavin T and Tri phosphonic corrosive presentations powerful movement against with least restricting energy and the RMSD esteems to be -5.75 Kcal/mol for Tri phosphonic acid, -4.96Kcal/mol for Thioflavin T and 2.0 Å. The examination of ligands in docking, empowered us to distinguish explicit buildups viz. Glu-11, Val-12, His-13 and His-14 inside the limiting pocket to assume a significant part in ligand restricting proclivity. Consequently, the proposed drugs were introduced to mainstream

researchers for additional investigational Confirmation. The consequences of the current investigation obviously showed the in silico molecular docking investigation of Chrysamine G, Curcumin, Thioflavin T and Tri phosphonic acid with protein displayed restricting connections and warrants further examinations required for the improvement of strong inhibitors for the treatment of AD.

Abbreviations

Alzheimer's disease- AD

Senile plaques- SPs

Amassed amyloid beta- Aβ),

Amyloid precursor protein – APP

Sporadic AD- SAD

Late-onset AD- LOAD

Familial AD- FAD

Presenilin-1- PSEN1

Presenilin-2- PSEN2

Neurofibrillary tangles- NFTs

Dystrophic neurites- DNs

Chrysamine-G- CG

aminotris(methylenephosphonic acid)- ATMP

cerebral amyloid angiopathy- CAA

Root mean square deviation of non-hydrogen atoms-RMSD

References:

1. Uddin M S, Al M A, Takeda S, Sarwar M S, & Begum M M (2018) Psychogeriatrics 19:1-8. https://doi.org/10.1111/psyg.12368

2. Al Mamun A, Uddin M S, Kabir M, Shahid S, Mathew B, Rauf A, Ahmed M & Ghulam A T (2020) Neurotox Res 38: 8-17. 10.1007/s12640-020-00185-1

3. M. F. Hossain H F, M. S. Uddin M S, Uddin G M S, Sumsuzzman D, Siddiqul I D, George E B, Mathew B & Ashraf G (2019) Molecular Neurobiology 56:8255-8276. https://doi.org/10.1007/s12035-019-01660-3.

4. Golde T E, Schneider L S & Koo E H (2011) Neuron 69:203-13. 10.1016/j.neuron.2011.01.002

5. Uddin M S, Hossain M F, Mamun A A, Shah M A, Hasana S, Bulbul I J, Sarwar M S, Mansouri R A, Ashraf G M, Rauf A, Abdel-Daim M M & Bin-Jumah M N (2020) Sci Total Environ 725:138313. https://doi.org/10.1016/j.scitotenv.2020.138313

6. Van Cauwenberghe C, Van Broeckhoven C & Sleegers K (2016) Genet Med. 18:421-430. 10.1038/gim.2015.117

7. Uddin M S, Al Mamun A, Asaduzzaman M, Hosn F, Abu Sufian M, Takeda S, Herrera-Calderon O, Abdel-Daim M M, Uddin G M S, Noor M A A, Begum M M, Kabir M T, Zaman S, Sarwar M S, Rahman M M, Rafe M R, Hossain M F, Hossain M S, Ashraful Iqbal M & Sujan M A R (2018) Ann Neurosci 25:25-37. 10.1159/000481812

8. Chakrabarti S, Khemka V K, Banerjee A, Chatterjee G, Ganguly A & Biswas A (2015) Aging Dis 6:282-299. 10.14336/AD.2014.002

9. Uddin M S, Kabir MT, Al Mamun A, Abdel-Daim M M, Barreto G E & Ashraf G M (2019) Mol Neurobiol 56:2450-2465. 10.1007/s12035-018-1237-z

10. Chu LW (2012) Hong Kong Med J 18:228-237. PMID: 22665688.

11. Sun X, Chen W D & Wang Y D (2015) Front Pharmacol 6:221. https://doi.org/10.3389/fphar.2015.00221

12. Uddin M S, Al Mamun A, Kabir M T, Jakaria M, Mathew B, Barreto G E & Ashraf G M (2019) Mol Neurobiol 56:4925-4944. doi: 10.1007/s12035-018-1420-2

13. Harilal S, Jose j, D. G. T. Parambi D G, Kumar R, Mathew G E, Uddin S, Kim H & Mathew B (2019) The Journal of Pharmacy and Pharmacology 71:1370-1383. 10.1111/jphp.13132

14. Uddin M S, Al M A, Labu Z K, Hidalgo-Lanussa O, Barreto G E & Ashraf G M (2019) Journal of Cellular Physiology 234:8094-8112. https://doi.org/10.1002/jcp.27588

15. Al Mamun A & Uddin M S, Comb Chem High Throughput Screen (2020) 23:836-841. 10.2174/1386207323666200117103144

16. Uddin M S, Rahman M M, Jakaria M, Rahman M S, Hossain M S, Islam A, Ahmed M, Mathew B, Omar U M, Barreto G E & Ashraf G M (2020) Mol Neurobiol 57:2654-2670. 10.1007/s12035-020-01911-8.

17. VanItallie T B (2017) Metabolism 69S:S41-S49. doi: 10.1016/j.metabol.2017.01.014.

18. Graeber M B, Li W & Rodriguez M L 585 (2011) FEBS Lett. 585:3798-3805. doi: 10.1016/j.febslet.2011.08.033.

19. Schneider J A, Arvanitakis Z, Leurgans S E & Bennett M D (2009) Annals of Neurology 66:200-208. https://doi.org/10.1002/ana.21706

20. Villemagne V L, Burnham S, Bourgeat P, Brown B, Ellis K A, Salvado O, Szoeke C, Macaulay S L, Martins R, Maruff P, Ames D, Rowe C C & Masters C L (2013) Lancet Neurol 12:357-367. doi: 10.1016/S1474-4422(13)70044-9

21. Bateman R J, Xiong C, Benzinger T L, Fagan A M, Goate A, Fox N C, Marcus D S, Cairns N J, Xie X, Blazey T M, Holtzman D M, Santacruz A, Buckles V, Oliver A, Moulder K, Aisen P S, Ghetti B, Klunk W E, McDade E, Martins R N, Masters C L, Mayeux R, Ringman J M, Rossor M N, Schofield P R, Sperling R A, Salloway S & Morris J C (2012) N Engl J Med. 367:795-804. DOI: 10.1056/NEJMoa1202753

22. Zaplatic E, Bule M, Shah S Z A, Uddin M S & Niaz K (2019) Life Sci 224:109-119. DOI: 10.1016/j.lfs.2019.03.055

23. Uddin M S & Kabir M T (2019) Front Cell Dev Biol 7:197. https://doi.org/10.3389/fcell.2019.00197

24. M. S. Uddin M S, Al M A, Jakaria S T, Thangapandiy S, Ahmade J, Rahman A, Mathew B, Mohamed M. A D & Aleya L (2020) Science of the Total Environment 707:135624. https://doi.org/10.1016/j.scitotenv.2019.135624

25. Alzheimer's Association (2017) Alzheimer's & Dementia 13:325-373. https://doi.org/10.1016/j.jalz.2017.02.001

26. Uddin M S & Rashid M (2020) Apple Academic Press. ISBN 9781771887977. Paperback ISBN: 978-1-77463-471-4.

27. Uddin M S (2016) Annals of Neurosciences 23:218-229. doi: 10.1159/000449482

28. Uddin M S, Kabir M T, Tewari D, Mathew B & Aleya L, Sci Total Environ, 700 (2020) 134836. https://doi.org/10.1016/j.scitotenv.2019.134836

29. Maia M A & Sousa E (2019) Pharmaceuticals (Basel) 12:1-31. https://doi.org/10.3390/ph12010041

30. Rahman MA, Rahman MR, Zaman T, Uddin MS, Islam R, Abdel-Daim MM & Rhim H (2020) Curr Pharm Des 26:772-779. https://doi.org/10.2174/1381612826666200107142541

31. Uddin M S, Kabir M T, Rahman M H, Alim M A, Rahman M M, Khatkar A, Al Mamun A, Rauf A, Mathew B & Ashraf G M (2020) Curr Pharm Des, 26:4690-4698. https://doi.org/10.2174/1381612826666200406075044

32. Chen, Gf, Xu, Th, Yan Y, Zhou Yr, Jiang Y, Melcher K & Xu H E (2017) Acta Pharmacol Sin 38:1205-1235. DOI: 10.1038/aps.2017.28

33. Paravastu A K, Leapman R D, Yau W M & Tycko R (2008) Proc Natl Acad Sci U S A 105:18349-18354. DOI: 10.1073/pnas.0806270105

34. Ribeiro A J M, Holliday G L, Furnham N, Tyzack J D, Ferris K & Thornton J M (2018) Nucleic Acids Res 46(D1):D618-D623. DOI: 10.1093/nar/gkx1012

35. Altschul S F, Madden T L, Schäffer A A, Zhang J, Zhang Z, Miller W & Lipman D J (1997) Nucleic Acids Res 25:3389-3402. DOI: 10.1093/nar/25.17.3389

36. Morris G M, Huey R, Lindstrom W, Sanner M F, Belew R K, Goodsell D S & Olson A J (2009) J Comput Chem 30:2785-3791. DOI: 10.1002/jcc.21256

37. Sanner M F (1999) J Mol Graphics Mod 17:57-61. PMID: 10660911.

38. DeLano W L (2002) The PyMOL molecular graphics system. San Carlos: DeLano Scientific.

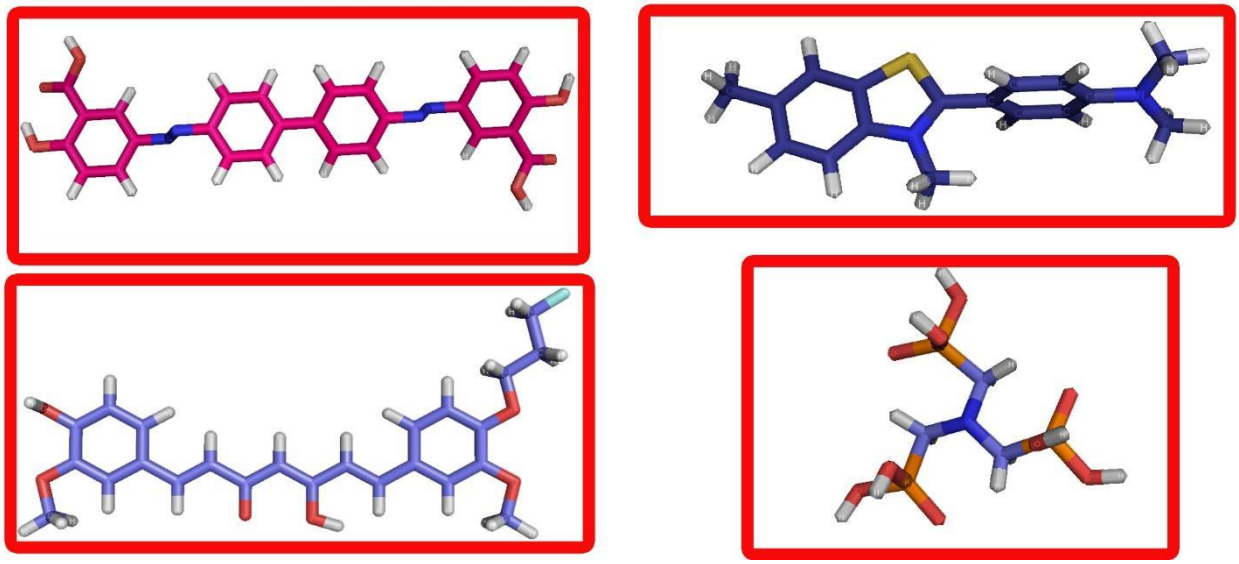

Fig. 1: 3-Dimensional structure of multiple ligands (Chrysamine G, Curcumin, Thioflavin T & Tri phosphonic acid) represented in stick form. The image was generated using Pymol.

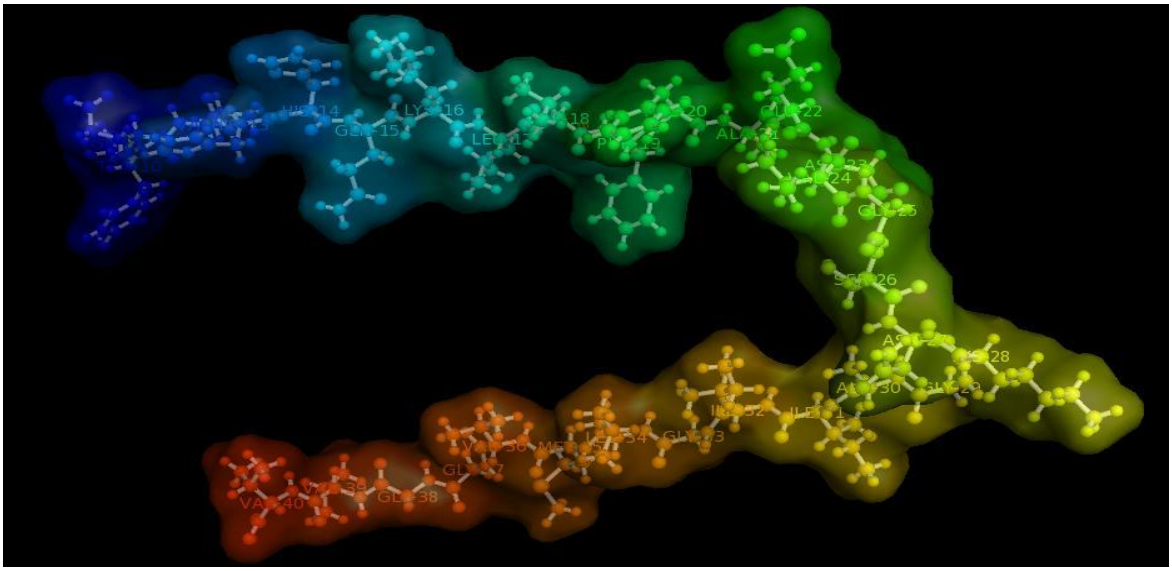

Fig. 2: 3-Dimensional structure of β-amyloid protein 2LMN represented in rainbow color surface along with ball & stick form. The image was generated using Pymol

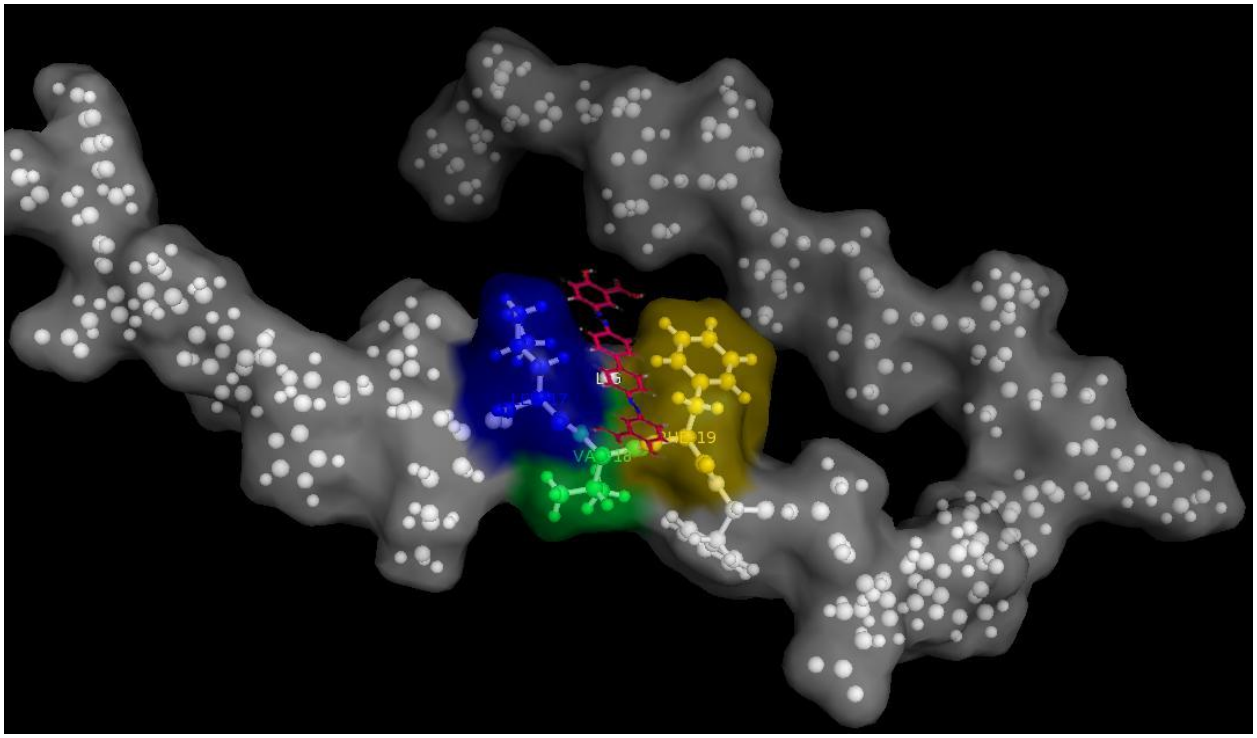

Fig. 3: Protein-Ligand docking interaction of Chrysamine G represented in stick form magenta color and β-amyloid protein 2LMN represented in ash color surface along with ball & stick form catalytic residues with rainbow colors. The image was generated using Pymol

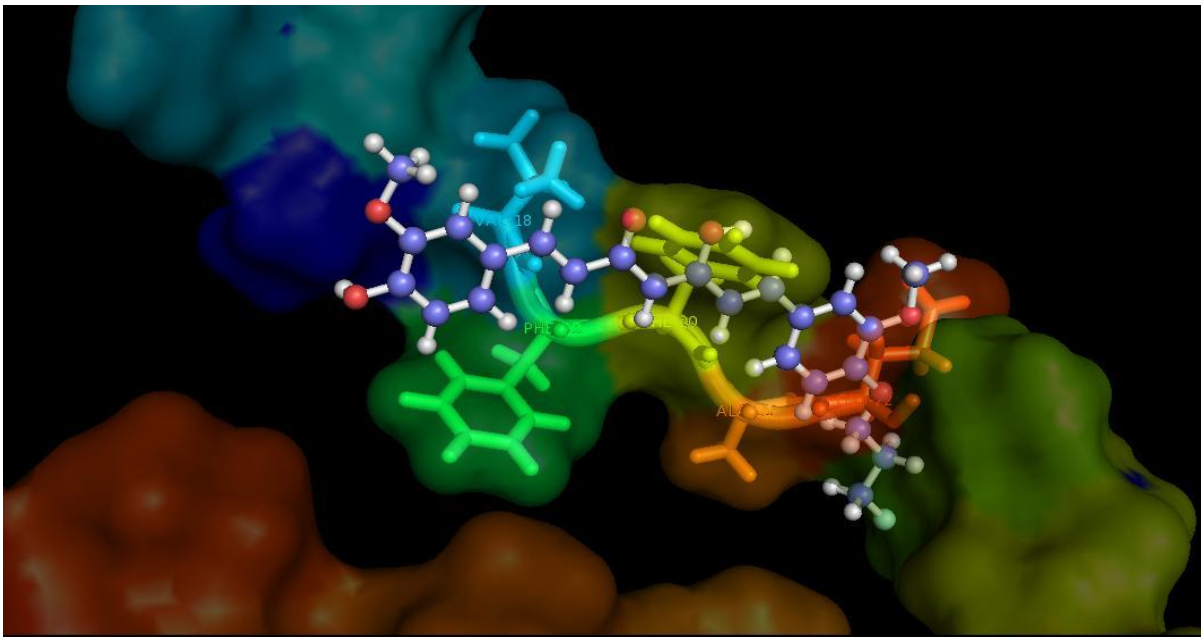

Fig. 4: Protein-Ligand docking interaction of Curcumin represented in ball & stick form, and β-amyloid protein 2LMN represented in surface, catalytic residues represented in stick form with rainbow colors. The image was generated using Pymol

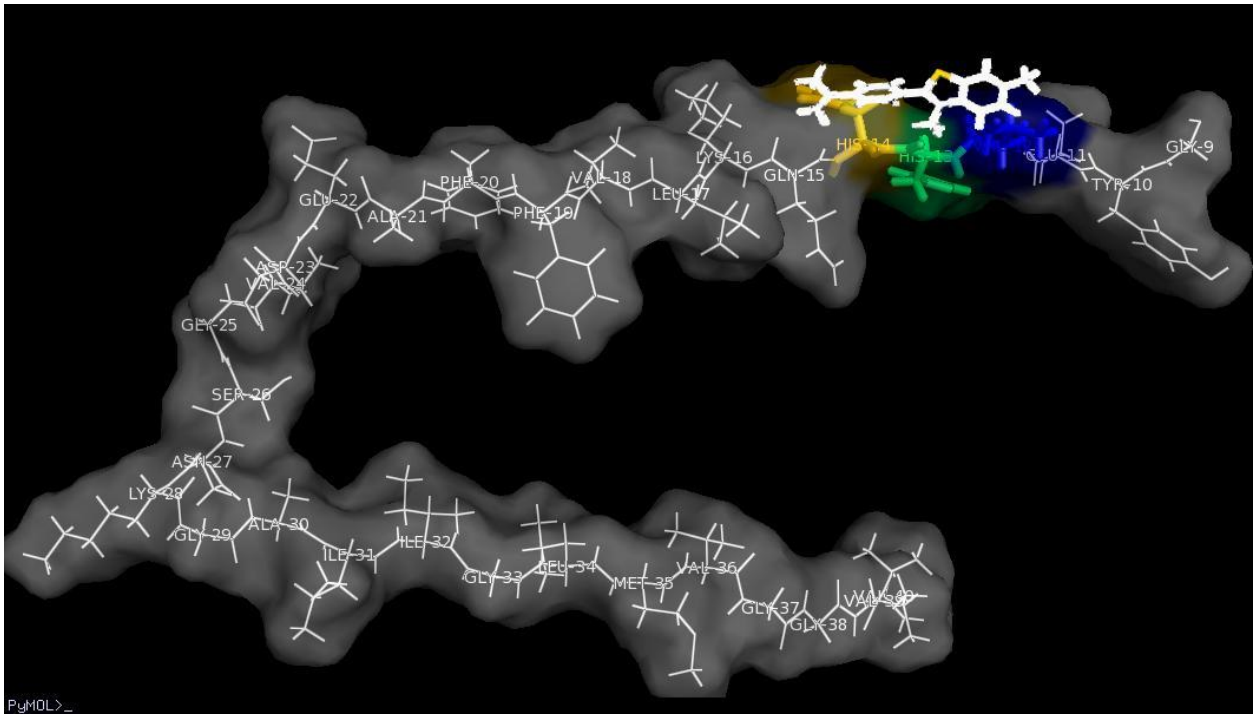

Fig. 5: Protein-Ligand docking interaction of Thioflavin T represented in stick form white color and β-amyloid protein 2LMN represented in ash color surface along with stick form, catalytic residues mentioned with rainbow colors. The image was generated using Pymol

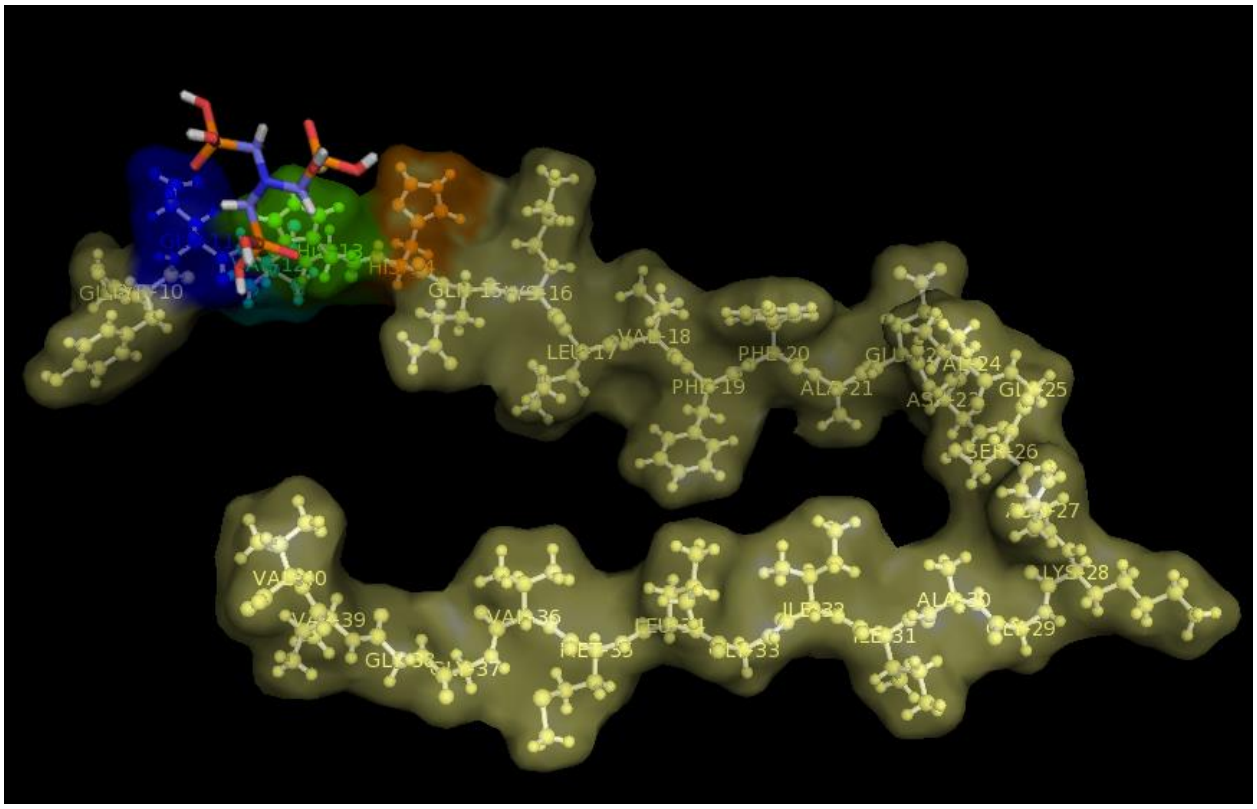

Fig.06: Protein-Ligand docking interaction of Tri phosphonic acid represented in stick form and β-amyloid protein 2LMN represented in light yellow color surface along with ball & stick form, catalytic residues mentioned with rainbow colors. The image was generated using Pymol